#### Research Article

Nabilah Afiqah Mohd Radzuan\*, Izzat Mat Samudin, Mohammad Reza Vaziri Sereshk, Quanjin Ma, Abu Bakar Sulong, Farhana Mohd Foudzi, and Nishata Royan Rajendran Royan

# A comprehensive approach for the production of carbon fibre-reinforced polylactic acid filaments with enhanced wear and mechanical behaviour

https://doi.org/10.1515/epoly-2025-0002 received January 20, 2025; accepted May 03, 2025

**Abstract:** Precise control of filament parameters, including material composition and printing orientation, enables the alignment of carbon fibres (CFs) in a single orientation in additive manufacturing processes. This study reveals that printing in 0° orientation enhances both tribological and mechanical properties in CF reinforced polylactic acid composites. By fabricating in-house filaments with CFs, superior flexural, impact, and tensile strength were achieved, with improvements of ~75% compared to conventional filaments. Findings also reveal that 0° orientation improves the printed layups in terms of interfacial bonding and adhesion within the layup sequence. It highlights the precise adjustment parameter in polymer composite filament with fibre filler, opening possibilities for advanced structures with integrated programmable functionalities in 4D printing applications.

**Keywords:** fused filament fabrication, polymer composites, orientation control, tribology properties, mechanical properties

Izzat Mat Samudin, Abu Bakar Sulong, Farhana Mohd Foudzi:
Advanced Manufacturing Research Group, Department of Mechanical & Manufacturing Engineering, Faculty Engineering & Built Environment, Universiti Kebangsaan Malaysia, 43600, Bangi, Selangor, Malaysia Mohammad Reza Vaziri Sereshk: Department of Engineering, Central Connecticut State University, New Britain, CT, 06050, United States of America

**Quanjin Ma:** School of System Design and Intelligent Manufacturing, Southern University of Science and Technology, Shenzhen, 518055, China **Nishata Royan Rajendran Royan:** School of Engineering, UOW Malaysia KDU University College, Glenmarie Campus, Shah Alam, 40150, Selangor, Malaysia

ORCID: Nabilah Afigah Mohd Radzuan 0000-0003-0859-6112

### 1 Introduction

Controlling the orientation during additive manufacturing is critical for tailoring the mechanical properties of a material. Prior studies have highlighted that aligned fibres within printed composites enhance loading capacity and reduce failures such as warping and poor interlayer adhesion (1). This alignment leverages the anisotropic behaviour of fibres, allowing for mechanical properties to be enhanced for specific applications (2). Conversely, studies using fused filament fabrication (FFF) indicate that orthogonal printing orientations (e.g., ZXY) can improve fracture toughness, achieving values as high as 1.97 MPa·m<sup>-2</sup>, despite weak inter-filament bonding due to misaligned fibres (3). However, orthogonal orientations may adversely impact wear resistance, with observed wear rate increases of 25-34% compared to perpendicular printing directions (4). Furthermore, fibre distribution and alignment significantly influence tribological performance, with severe fibre breakage contributing to higher wear rates in perpendicular orientations (5-7). Wear resistance is particularly crucial for applications involving moving such as robotic joints and automotive components, which demand materials to endure friction and mechanical stress without significant wear.

Fibre orientation, referring to the arrangement of long segments with a high length-to-diameter ratio, plays a pivotal role in dictating the properties of composite structures. While it is acknowledged that fibres within a polylactic acid (PLA) matrix may exhibit random orientation due to limitations in compound mixing, precise control of filament parameters, such as extrusion speed and layer thickness, can align carbon fibres (CFs) longitudinally during fabrication (8). Evidence reveals that fibres are predominantly oriented along the filament axis when parameters are optimized (9). Surface roughness suggests unevenness due to fibre segments; this may stem from the interaction of fibre length and filament diameter during extrusion (10). These findings align with the assertion that carefully controlled

<sup>\*</sup> Corresponding author: Nabilah Afiqah Mohd Radzuan, Advanced Manufacturing Research Group, Department of Mechanical & Manufacturing Engineering, Faculty Engineering & Built Environment, Universiti Kebangsaan Malaysia, 43600, Bangi, Selangor, Malaysia, e-mail: afiqah@ukm.edu.my

extrusion processes reduce defects and enable consistent fibre orientation.

Apart from printing and fibre orientation, the materials themselves play a pivotal role in determining mechanical performance and suitability for specific applications. PLA, a biodegradable thermoplastic polymer derived from renewable resources, was selected for this study due to its compatibility with additive manufacturing processes (11). Commercially available PLA was evaluated against the synthetic polymer polyamide (PA), focusing on their mechanical properties when applied to additive manufacturing using FFF. While thermoplastic materials mainly exhibit similar mechanical performance, it is important to note that PA offers higher strength and heat resistance. However, PLA is easier to process, making it more suitable for additive manufacturing. A recent study on the additive manufacturing of PLA demonstrated its excellent mechanical performance, with tensile strength ranging from 26 to 33 MPa as the nozzle temperature increased to 230°C (11). These results indicate that PLA exhibits excellent fixity while maintaining its mechanical strength at an optimal level, making it suitable for 4D printing and shape memory polymer technology (12). Thus, to enhance performance and mechanical strength, additive fillers such as CF are commonly incorporated into the PLA matrix, which is applied in applications requiring high precision and durability, such as robotics. Notably, this study emphasizes PLA reinforced with CF due to its potential in 4D printing applications, where the material's shape memory properties and low stretchability are crucial (13). This highlights the need for advanced materials capable of maintaining structural integrity while meeting functional demands.

PLA/CF composites have been widely studied and are commercially available from brands such as Flashforge 3D Technology (14), Stampa3DSud (15), Ultimaker (16,17), and others. However, commercial filaments often demonstrate limitations on the mechanical performance due to limited variations in material formulations. For example, studies with 15 wt% CF compositions have reported average tensile strengths for PLA reinforced with CF ranging from 14 to 22 MPa (17). Additionally, pure PLA filaments of different colours exhibit variability in tensile strength, with black PLA demonstrating the highest strength (34 MPa) and green PLA the lowest (28 MPa) (15). Such findings highlight the limitations of commercial filaments, where additives like talc are either absent or not homogeneously distributed in the polymer formulations, adversely affecting filament performance.

Based on these findings, it is evident that custom-made filaments play a critical role in achieving optimal mechanical performance in 3D-printed parts, particularly when combined with high-quality printing parameters. Additionally, integrating additive manufacturing with multi-physics finite-element analysis has proven to significantly enhance the fabrication of

advanced multi-materials for diverse applications, including biological piezoelectrics, sensor devices, and concrete structures (6,18,19). Furthermore, precise control of the printing layup sequences has been shown to improve material stiffness and strength. However, existing research on printed composite samples using the FFF technique highlights a notable limitation in which the toughness of materials printed in the 90° direction tends to deteriorate compared to those printed in diagonal orientations (20). This is attributed to internal fibre loading, which often results in the reorientation of fibres toward the loading direction. Such reorientation increases elongation and induces more ductile behaviour.

Therefore, improved understanding of the surface characteristics of printed samples is critical, as both micro and macro defects can compromise adhesion within the layup and degrade mechanical performance. Enhancing mechanical performance in printed polymeric composites can be achieved through controlled thermal processing. For instance, introducing heat during fabrication has been shown to minimize voids and improve interlayer adhesion (21). Studies on conventional nylon-6 (polyamide) materials demonstrated that temperature increments enhance tensile strength by up to 45%, as moisture content is effectively reduced (22). However, an alternative study highlighted that excessively high printing temperatures could lead to an increase in porosity (up to 39%), which adversely affects stiffness, strength, and elongation at break (23). These findings highlight the importance of understanding balanced temperature parameters to enhance performance, especially when fabricating own filament.

Conventional filaments have been extensively studied; however, their customization potential to enhance mechanical performance remains limited. Unlike commercial filaments, in-house fabricated filaments enable tailored properties, providing greater control over mechanical and printing parameters. Research into conventional filaments has explored lattice structures and their integration into 4D printing technologies (24). For instance, studies using conventional filament by Markforged, United States, successfully printed and analysed hexagonal frame parts, emphasizing complexity over lattice and grid structures (25). Despite these advances, only a few studies focus on in-house fabricated filaments, which suggest that customized filaments offer superior mechanical control, particularly in lattice structures. By fabricating filaments with controlled fibre orientations, it becomes possible to enhance interfacial bonding and mechanical properties. In this study, a comprehensive approach is adopted to produce novel in-house PLA/CF filaments by combining reinforcement through varying CF compositions, printing parameters, and precise print orientation control. The filaments were produced using a controlled extrusion process, ensuring consistent fibre alignment and minimizing defects like voids or delamination.

These custom-made filaments exhibit enhanced tribological and mechanical properties, outperforming commercial counterparts. This study evaluates these properties through surface characterizations, friction and wear analysis, and mechanical testing under various temperature conditions, aiming to address the limitations of conventional filaments and expand their application potential.

no temperature exposed. The CF, with an average diameter of 9  $\mu$ m, an aspect ratio of 43, and a density of 1.75 g·cm<sup>-3</sup>, was used in this study (11,13). The conventional filament used for comparison was the PolyLite PLA brand by Polymaker, purchased from Pebblereka Sdn. Bhd.

## 2 Materials and methodology

#### 2.1 Materials

The samples for this study were printed using a Funmat High Temperature (HT) printer, with the filament prepared to a diameter of 1.75 mm. The filament was fabricated using compound materials consisting of PA grade PA2200 and PLA that served as the matrix polymer. Both polymers, with densities of 0.45 g·cm<sup>-3</sup> for PA and 1.24 g·cm<sup>-3</sup> for PLA, were supplied from Sigma Aldrich Sdn. Bhd. To enhance the mechanical and tribological properties, the PLA matrix was mixed with CF (grade CFP-7-50) supplied by Shenzhen Yataida High-Tech. Co. Ltd. (Shenzhen, China). This mixing was conducted using an IKA mixer propeller stirrer (model RW20 WERK) at a controlled speed of 300-500 rpm for 5 min. Although fibres with a high aspect ratio may experience breakage and shortening during this process, the controlled stirrer speed ensured homogeneity while minimizing fibre breakage, resulting in acceptable fibre lengths ranging from 200 to 300 µm with

#### 2.2 Sample preparations

The compound materials were prepared with CF compositions of 5, 9, and 12 wt% to analyse the effects of CF content on wear resistance and mechanical strength compared to pure PA and PLA. Before processing, all materials were dried in a vacuum oven (Thermo VY 6060M) at 70°C for 5 h to eliminate moisture, which could otherwise lead to voids and failure during filament production due to entrapped bubbles (26,27). This drying process significantly improves filament quality. The dried compound materials were fed into a 3Devo Filament Maker (450 series) set to an extrusion speed of 3.6 rpm and subjected to varying temperatures across four heating zones (170°C, 190°C, 180°C, and 110°C). These temperatures were optimized to ensure uniform cooling and solidification of the filament, maintaining a consistent diameter of 1.75 mm, as shown in Figure 1a-c. Note that the CF is extruded through the filament maker nozzle, aligning into specific orientations as it becomes surrounded by melted PLA resin. The detailed process of achieving specific orientations during printing is depicted in Figure 1d. The filament was either immediately used for printing or dried again for a minimum of 5 h if printing was delayed. Samples were printed using a Funmat HT printer employing the FFF

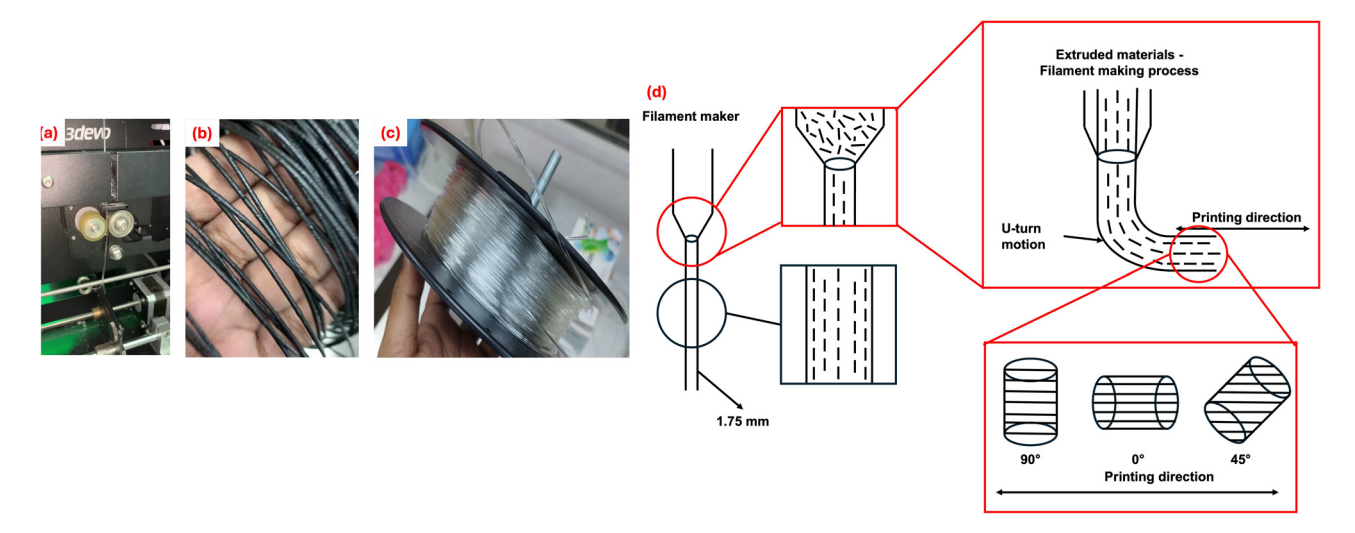


Figure 1: (a) Visual representation of filament preparations using 3Devo filament maker, (b) Prepared in-house PLA/CF filament, (c) PLA in-house filament, and (d) illustrations on printing process to obtain specific orientations.

technique. The printer settings included a nozzle temperature of 230°C, a bed temperature range of 90–110°C, a print speed of 50 mm·s<sup>-1</sup>, and a layer height variation between 0.1 and 0.3 mm. The bed temperature varies depending on the room temperature conditions in order to avoid warping issues. The prepared filaments were categorized into two types: conventional filaments (commercially available Poly-Lite PLA from Polymaker) and customized filaments produced in-house.

# 2.3 Characterisations of PLA, PA, and PLA/CF printed samples

The rheological behaviour of the compound materials was analysed using a rheology machine (Shimadzu CFT-500EX) to evaluate the flow properties that are critical during additive manufacturing. Data were recorded using CFT-500EX software at a set temperature of 200°C and a constant load of 40 N. Thermal and dynamic properties were analysed using a Mettler Toledo machine. Thermogravimetric (TG) analysis and differential scanning calorimetry were conducted in a nitrogen environment set between 30°C and 900°C, with a heating rate of 20°C·min<sup>-1</sup>, adhering to ASTM E1131-98 standards (28).

Wear analysis was performed using a pin-on-disk apparatus in accordance with ASTM G99-95a to evaluate

the tribological performance of PLA and PLA/CF printed samples. The samples were cylindrical with a diameter of 8 mm and a height of 15 mm, and flat ends were pressed onto a rotating flat circular disk made from stainless steel as shown in Figure 2b. Sliding speeds of 0.4, 0.8, and 1.2 m·s<sup>-1</sup> were tested for a total sliding distance of 1,000 m. The frictional tests were conducted at a load of 100 N, and the frictional behaviour was monitored using a rotary torque sensor, with data acquisition via an IMC A/D data logger. The frictional force was calculated by dividing the recorded torque values by the effective radius of the disk (77 mm). To ensure consistency and reliability, each test condition was repeated five times under identical parameters and standards. Previous studies indicate that excessive frictional heat generated at higher sliding speeds can lead to deformation of polymer surfaces (29). This deformation affects the wear performance by altering the surface topology and inducing microstructural changes.

The photoluminescence (PL) properties of the samples were investigated using a PL spectrometer (Edinburgh Instrument, model FLS920) with an excitation wavelength range of 350–680 nm and a slit width of 5.0 nm. The surface characteristics of the wear samples were analysed using atomic force microscopy (AFM, model NX-10, Park Systems). AFM measurements were conducted at a resonant frequency of 10.5 kHz using scanning electron microscopy. The topological behaviour of the printed samples, oriented in various directions, was evaluated at room temperature. A small scan area of 15  $\mu$ m was selected for

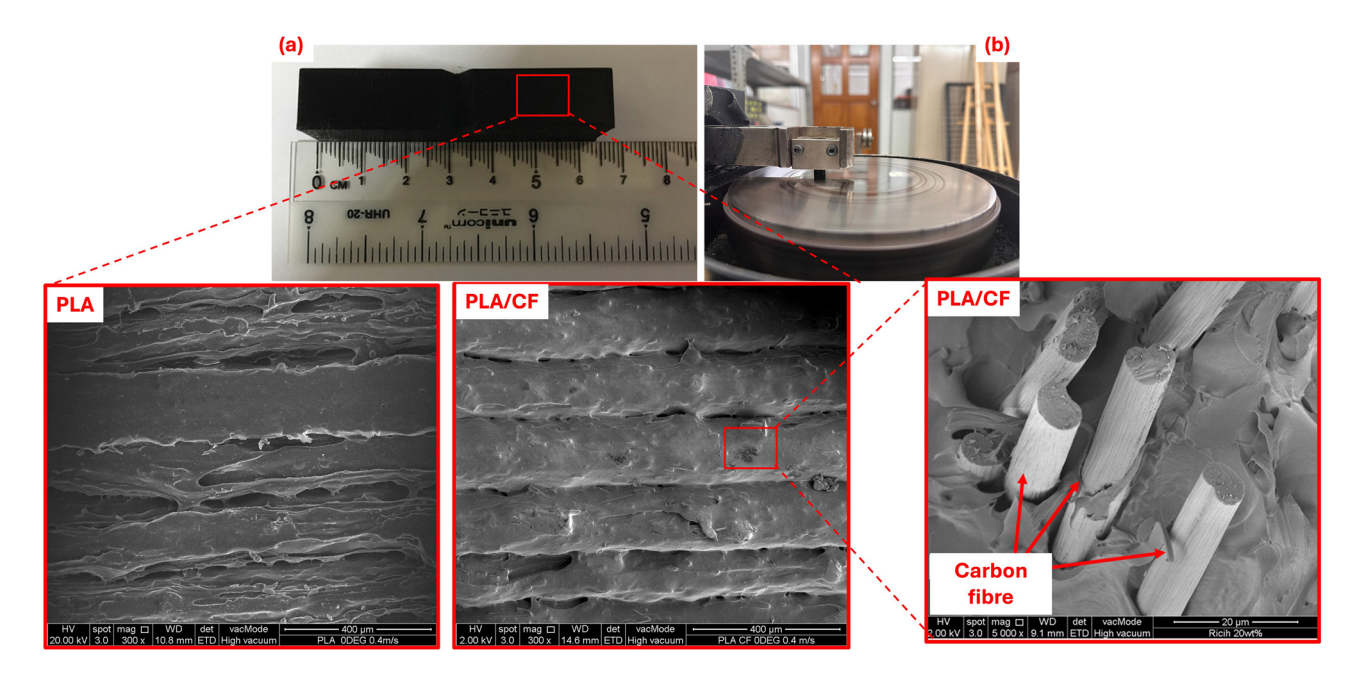


Figure 2: (a) Example of the printed PLA/CF sample impact test and enlarged microscopic images of PLA and PLA/CF samples of its cross-sectional area and (b) PLA/CF samples following ASTM G99-95a for pin-on-disk testing.

detailed surface roughness analysis, aligning with recommendations from a prior study (30). Additionally, field emission scanning electron microscopy (model Merlin, Zeiss) was utilized to study the topology and morphological characteristics of the samples prepared for mechanical testing.

To evaluate the mechanical performance of the structural materials, a comprehensive series of tests including tensile, flexural, compression, and impact tests was performed using a universal testing machine (UTM, Instron 5567, 30 kN). For tensile testing (ASTM D638-99), the crosshead speed was set at 5 mm·min<sup>-1</sup> with tests conducted across a temperature range of 30-200°C. Similarly, the flexural test (ASTM D790) employed a speed of 1 mm·min<sup>-1</sup> and a support span of 72 mm. Compression tests (ASTM D3410) were carried out at environment temperatures from 30°C to 120°C. Impact testing followed ASTM D256-19 standards using an Izod pendulum with an energy value of 50 J under room temperature conditions. The prepared samples are illustrated in Figure 2a. The densification of PLA/CF composites was assessed in accordance with ASTM D792, utilizing standard level balance, specifically the Mettler Toledo ME-T analytical balance, and distilled water with a density of 0.998 g·cm<sup>-3</sup>. As shown in the micrograph images of Figure 2a, the prepared filament, extruded by the filament maker, has been successfully fabricated without any fibre pull-out or exposure on the filament surface. This is crucial for improving the adhesion bonding between printed layers, as reflected in the mechanical properties data reported in this study.

## 3 Results and discussion

## 3.1 Thermogravimetric and rheological analysis

PLA and PA exhibit viscoelastic behaviour that significantly affects the processability of filament fabrication and the printability of manufactured parts (31). Rheological analysis is therefore essential in evaluating polymeric composites, and PLA/CF was analysed at varying material compositions as shown in Figure 3a. Shear rates influence the dynamics within the print nozzle. The reported data of PLA/CF composites demonstrated pseudoplastic behaviour with viscosity decreasing as the shear rate increased. Higher filler compositions, specifically 9 and 12 wt%, exhibited greater viscosity and shear rate compared to 5 wt%. However, the 9 wt% composition exhibited enhanced shear thinning behaviour compared to 12 wt% due to a poor network structure within the compound composites. This observation is attributed to weaker interfacial bonding within the polymeric particles caused by higher filler compositions (32), which was evident in the smoother surface finish of PLA compared to PLA/CF as can be seen in Figure 2a. Additionally, the critical shear rate for the onset of shear thinning differed significantly by a factor of 6 between 5 and 9 wt% compositions. To further substantiate these findings, the shear thinning behaviour was modelled using the Carreau-Yasuda equation (Eq. 1) and the power-law model (Eq. 2):

$$\eta(\dot{\gamma}) = \eta_{\infty} + (\eta_{0} - \eta_{\infty})(1 + (\lambda \dot{\gamma})^{a})^{\frac{n-1}{a}} \tag{1}$$

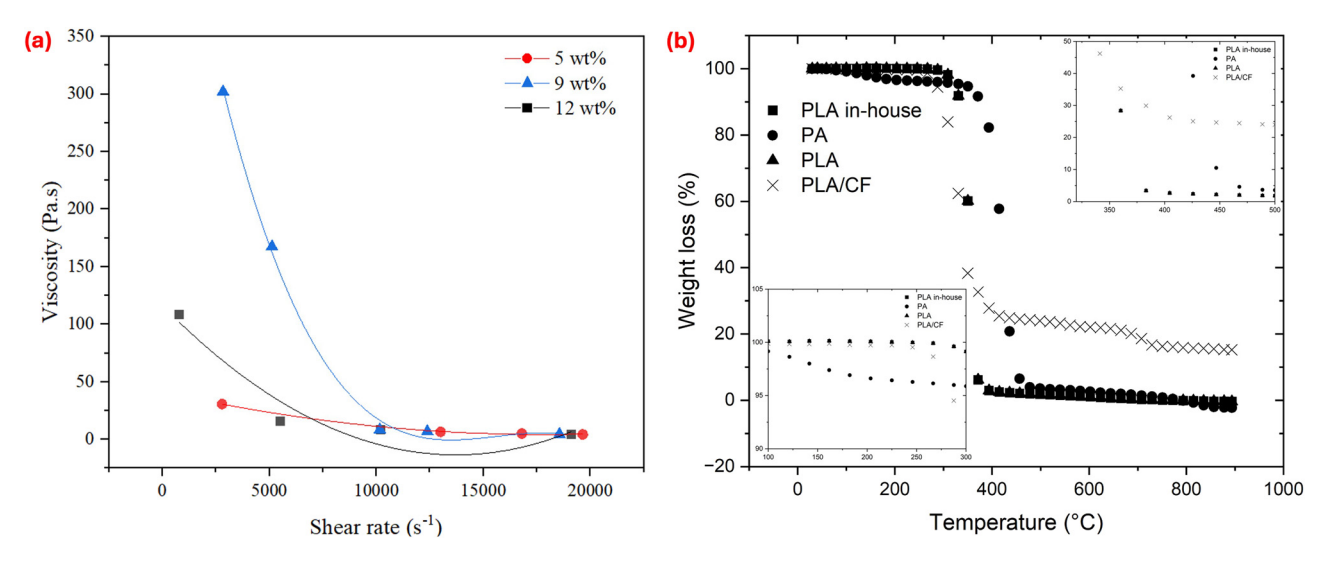


Figure 3: (a) Rheological analysis of PLA-reinforced CF at various compositions of 5, 9, and 12 wt%; (b) TG analysis of PLA, PA (as reference materials), and PLA-reinforced CF.

$$\eta(\dot{\gamma}) = K(\dot{\gamma})^{n-1} \tag{2}$$

The Carreau-Yasuda model quantified critical rheological parameters, where  $\lambda$  is the natural time, n is the power-law index,  $\eta_{\infty}$  is the infinite-shear-rate viscosity,  $\eta_0$ is the zero-shear rate viscosity,  $\dot{y}$  is the critical shear rate, and K is the consistency index. These parameters are essential for understanding the shear-thinning behaviour and transitioning between Newtonian and non-Newtonian states in composite materials. Prior studies on polymeric additive manufacturing and PLA filament making highlighted that the Newtonian plateau is controlled using the power-law region in the Carreau-Yasuda model, and it is used to determine viscosity curves through rheometric measurements (31). The critical shear rate  $(\dot{y}_{cr})$  determined by the Carreau-Yasuda model reveals the onset of shearthinning behaviour, while the critical shear stress  $(\tau_{cr})$ denotes the transition from Newtonian to non-Newtonian behaviour, as presented in Table 1. A notable observation in this study was the influence of CF composition on rheological properties. Specifically, the 5 wt% composition exhibited the lowest zero-shear viscosity, with an 85% increase in viscosity, demonstrating a clear trend in Figure 3a. The addition of 9 wt% CF resulted in a more pronounced shear-thinning behaviour, attributed to the destabilization of the network structure within the composite. Changes in flow behaviour at 9 wt% also transitioned from Newtonian to non-Newtonian states due to increased filler content and attributed to the presence of macromolecules with varying molar masses (33).

The TG analysis profiles of pure PA, PLA, in-house PLA, and PLA-reinforced CF are illustrated in Figure 3b. The nonisothermal behaviour of all materials exhibited a gradual weight loss decrement, starting at 295°C for PLA

**Table 1:** Rheological parameters of the Carreau–Yasuda model for PLA/CF

wt%	$\eta_0$ (Pa s)	$ au_{ m cr}$ (Pa)	n (-)	λ	$\dot{\mathcal{V}}_{\mathrm{cr}}$
5	45	0.018	0.000154	2,500	0.0004
9	300	0.06	0.9848	5,000	0.0002
12	110	0.063	0.00519	1,750	0.00057

materials, while PA materials exhibited a decrease beginning at 120°C. The weight loss at high temperatures is primarily attributed to intensive combustion and oxygen chemisorption, which forms surface oxygen-containing complexes (34). Notably, Figure 3b reveals that PLA/CF retained a significantly higher residual weight (approximately 40%) compared to pure polymer material, attributed to the introduction of CF reinforcement. However, excessive fibre content can diminish material stability due to weaker interfacial bonding (35). It is also noteworthy that the inclusion of PA materials provided a reference for thermal behaviour compared with PLA and PLA/CF. Although TG analysis data for PA materials were limited due to insignificant flexural test results, the comparison is valuable for context.

# 3.2 Wear and friction analysis of in-house prepared filament

The friction coefficient of PLA and PLA/CF composites was investigated, as summarised in Table 2. It was observed that the friction coefficient initially increased with sliding speed, reaching a peak at 0.8 mm·s<sup>-1</sup>, before decreasing at 1.2 mm·s<sup>-1</sup>. This reduction is attributed to the rise in interface temperature due to increased contact pressure, which softened the polymeric composite surface area specifically for PLA 45°, PLA 90°, PLA CF 0°, and PLA CF 90°. Consequently, the softened surface area reduced the shear forces required to break adhesion bonds within printed samples, thereby lowering the friction coefficient. Similar trends were observed in studies on printed PLA polymers by Zhiani Hervan et al. (29). However, a contrasting phenomenon was noted where an increase in sliding speed from 0.4 to 0.8 mm·s<sup>-1</sup> led to higher friction coefficients. This was due to layer deformation under increased contact pressure, caused by the compression of the sample layer's thickness, resulting in greater resistance to sliding.

Data from Table 2 indicate that the friction coefficient for PLA/CF printed at a 45° orientation increases steadily with higher sliding speeds. This increase is attributed to

Table 2: Coefficient of friction of in-house polymeric composites

Sliding speed (mm·s <sup>-1</sup> )	PLA 0°	PLA 45°	PLA 90°	PLA CF 0°	PLA CF 45°	PLA CF 90°
0.4	0.273 ± 0.11	0.216 ± 0.09	0.265 ± 0.12	0.332 ± 0.05	0.317 ± 0.06	0.276 ± 0.01
0.8	$0.202 \pm 0.007$	$0.355 \pm 0.02$	$0.374 \pm 0.03$	$0.419 \pm 0.06$	$0.393 \pm 0.07$	$0.354 \pm 0.06$
1.2	0.295 ± 0.08	0.161 ± 0.03	$0.324 \pm 0.04$	0.361 ± 0.09	0.397 ± 0.08	$0.313 \pm 0.06$

the presence of CF within the composite, which disrupts the layer cohesion by causing fibre pull-out at the edges of printed parts. Loads applied perpendicular to the 45° printing direction worsen these tribological issues due to uneven load transfer across the layers. This indicates that layers printed at a 45° orientation lack sufficient loadbearing support, leading to non-uniform stress distribution and increased wear evenly (36). Similar deformation trends were observed in continuous fibre-reinforced composites, where energy absorption shifted from folding deformation to bending deformation before failure (37). Interestingly, PLA printed at a 45° orientation exhibits a lower friction coefficient compared to PLA/CF at the same orientation, as the absence of CF avoids interfacial disruptions. While the addition of fillers like CF generally improves mechanical performance, its effectiveness strongly depends on the printing orientation. For PLA printed at 0°, there is an early instability during the running-in phase, which is caused by the irregular surface contact with the stainless-steel disk, resulting in inconsistent performance. This stage, characterized by uneven surface conditions, has been identified in tribological studies as the running-in phase, followed by fluctuation and stable friction phases (38). At higher sliding speeds (from 0.8 to 1.2 mm·s<sup>-1</sup>), the friction coefficient increased significantly, likely due to heightened frictional forces and shear stresses. These observations emphasize the critical role of controlled fibre alignment and surface uniformity in

improving wear resistance and overall performance for different printing orientations.

Figure 4a and b illustrate the impact of printing orientation on wear behaviour, with the 45° orientation showing moderate rates of height and weight loss under both moderate and high sliding speeds. The orientation angles were aligned with the printing direction of the CF, classified as 0°, 45°, and 90°, as depicted in Figure 4c. Samples subjected to higher sliding speeds experienced a stick-slip phenomenon that contributed to reduced wear (38). Tribological testing revealed significant differences between the 0° and 90° orientations, where PLA/CF at 90° exhibited greater wear, evidenced by the highest weight and height loss of about 0.19 g and 5.5 mm, respectively. The 3D-printed PLA/ CF samples, incorporating high-aspect-ratio fibres, exhibited an uneven surface due to fibre pull-out. This phenomenon contributed to increased wear rates in the composite samples, as evidenced by Figure 4b, which highlights greater weight loss in composite conditions compared to pure PLA. However, the tribological effects, as captured through optical imaging, revealed reduced wear for PLA/ CF composites at lower sliding speeds (0.4 and 0.8 m·s<sup>-1</sup>) compared to pure PLA, as illustrated in Figure 5. When comparing pure PLA, it experienced greater wear at 0° compared to 90° at higher sliding speeds (1.2 m·s<sup>-1</sup>), likely due to increased contact pressures causing material deformation and softening as the temperature increased (7). This thermal softening led to adhesion and transfer film

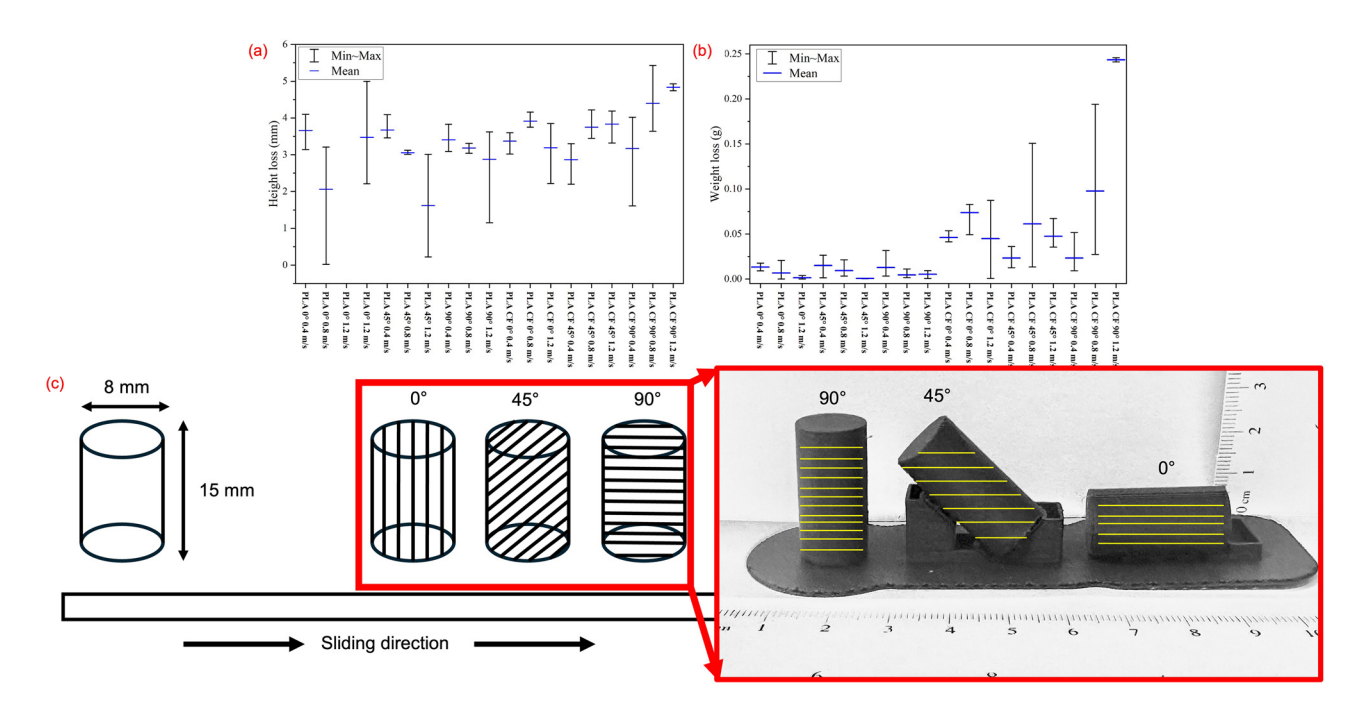


**Figure 4:** Tribological analysis of in-house PLA and PLA/CF through (a) height loss, (b) weight loss analysis, and (c) illustrations of tribological analysis and their actual printing samples with a yellow line indicating the printing orientation.

formation, which dominated the wear mechanism rather than the abrasion phenomenon. Controlling printing orientation, particularly at 0°, improved stress distribution and enhanced material performance relative to other printing orientations. Despite experiencing height and weight loss due to frictional heat, samples printed at 0° demonstrated favourable friction coefficients, as presented in Table 2. These findings provide critical insights into the tribological performance of in-house fabricated filaments, particularly for applications in 4D printing technologies that involve various deformations.

The findings in Figure 5 were supported by micrograph images and EDX mapping in Figure 6, which reveal the effects of sliding speeds on wear performance. At a higher sliding speed of 1.2 m·s<sup>-1</sup>, fibre pull-out in PLA/CF samples results in voids within the printed layup, leading

to reduced mechanical performance and an increase in the coefficient of friction. This can be attributed to the lower Sq value of surface roughness, which was recorded at 0.049 for PLA/CF at higher speeds compared to pure PLA under similar conditions, which can be seen in Table 3. EDX mapping demonstrated that the fibres were homogeneously even and distributed throughout the in-house fabricated filament, ensuring consistent properties. However, it was observed that fibre at higher loading caused a bumpy, rough structure, especially as the fibre became nearer the wall surface (11). At a lower speed of 0.4 m·s<sup>-1</sup>, PLA/ CF samples printed at 0° exhibited rougher surfaces (Sq = 0.2215), while in-house pure PLA samples showed smoother surfaces (Sq = 0.0628). Although layer gaps in printed layups observed in EDX mappings suggested potential delamination and warping during cooling, the ability to align



**Figure 5:** Overview of the wear samples through the optical images depending on the wear ability of the materials at different sliding speeds of 0.4, 0.8, and  $1.2 \, \mathrm{m \cdot s^{-1}}$ .

and orient fibre within the filament in a single direction during printing was validated, as shown in Figure 6. For both PLA and PLA/CF at 0° orientation, the elemental mappings reveal no significance differences, indicating even distribution of CF within the PLA matrix. These findings provide crucial insights into ensuring consistent mechanical properties and wear resistance in additively manufactured composites, which can be further analysed.

## 3.3 Surface roughness analysis of printed inhouse filament

To understand the impact of different orientation angles on the behaviour of printed layers, PL analysis was conducted, as illustrated in Figure 7a and b. The 0° orientation exhibited superior PL behaviour with higher intensity compared to 45° and 90° orientations for both pure PLA and PLA/CF materials. Specifically, the PL intensity for pure PLA at a wavelength of 425 nm is 6,119, whereas PLA/CF recorded a reduced intensity of 5,310, attributed to the addition of CF. This indicates that aggregationinduced emission phenomena can lead to brittleness in PLA composite samples (39). The dense structure of PLA/ CF has been identified as a factor causing lower light energy absorption and emission during PL testing, which contributes to its lower intensity (40). Table 4 shows the density data of printed filament at various thicknesses, supported by data obtained by PL properties. It shows that the layer thickness influenced the PL wavelength, with PLA/CF showing an increase up to 435 nm compared

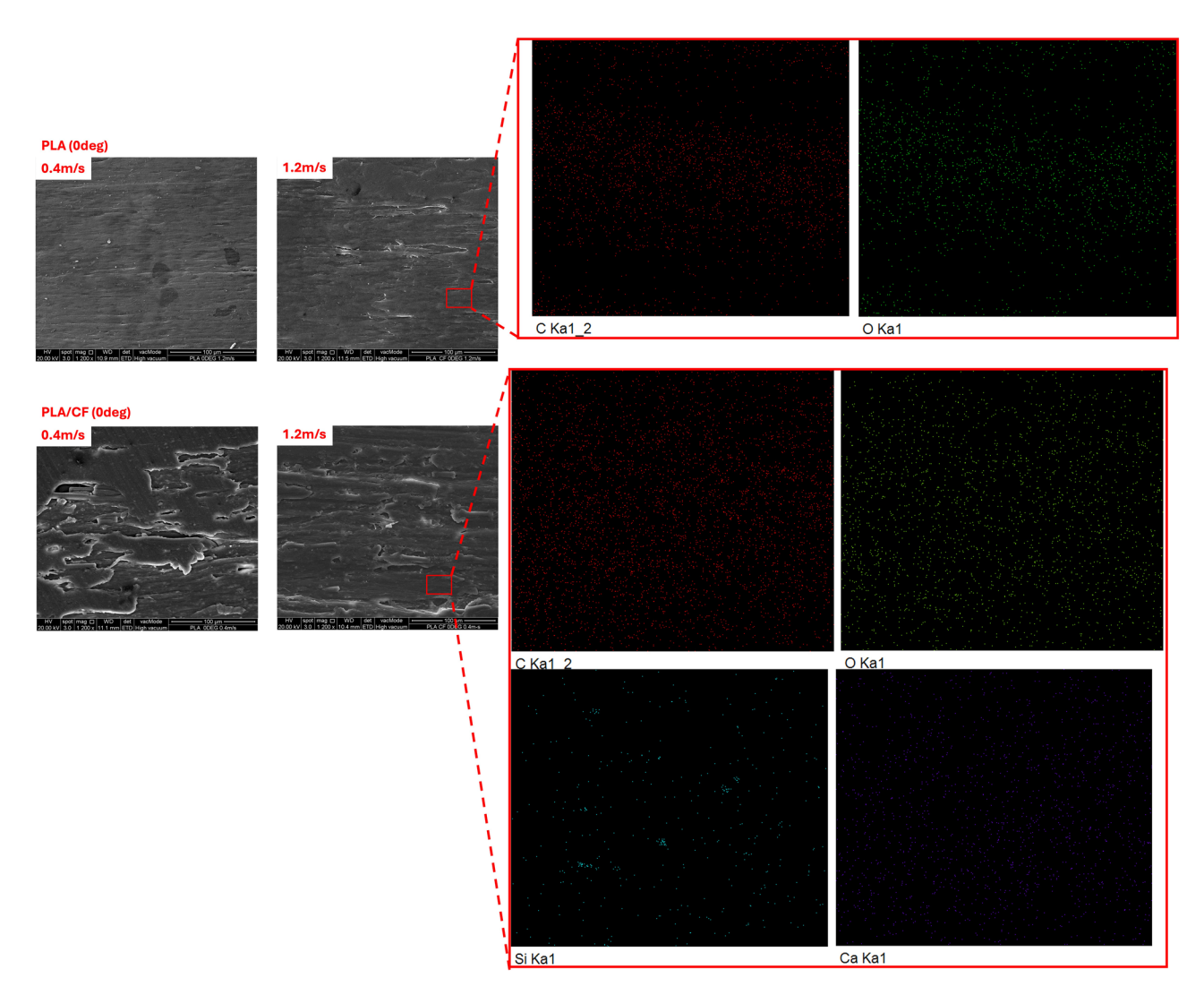


**Figure 6:** Micrograph images of in-house PLA and PLA/CF at 0° for different sliding speeds as well as their EDX mapping. The arrow indicates the direction of fibre within the filament.

Table 3: Surface roughness of PLA and PLA/CF samples for different printing orientations and sliding speeds

FFF printed sample	Sq μm Root mean square height	Sp µm Maximum peak height	Sv µm Maximum pit height	Sz μm Maximum height	Sa μm Arithmetical mean height
PLA 0° 0.4 m·s <sup>-1</sup>	0.0628	0.2756	0.2016	0.4771	0.0491
PLA 0° 0.8 m·s <sup>-1</sup>	0.2282	1.6107	0.6355	2.2461	0.1816
PLA 0° 1.2 m·s <sup>-1</sup>	0.1999	0.6088	0.6242	1.233	0.156
PLA CF 0° 0.4 m·s <sup>-1</sup>	0.2215	0.9707	0.8288	1.7995	0.176
PLA CF 0° 0.8 m·s <sup>-1</sup>	0.0957	0.36	0.5035	0.8634	0.0755
PLA CF 0° 1.2 m·s <sup>-1</sup>	0.049	0.1642	0.5443	0.7085	0.0343
PLA 90° 0.4 m·s <sup>-1</sup>	0.1685	0.5647	0.4535	1.0182	0.1358
PLA 90° 0.8 m·s <sup>-1</sup>	0.0864	0.3121	0.4203	0.7324	0.067
PLA 90° 1.2 m·s <sup>-1</sup>	0.0732	0.704	0.2731	0.5435	0.0571
PLA CF 90° 0.4 m·s <sup>-1</sup>	0.0852	0.2768	0.2347	0.5115	0.0673
PLA CF 90° 0.8 m·s <sup>-1</sup>	0.1366	0.818	0.4975	1.3155	0.0969
PLA CF 90° 1.2 m·s <sup>-1</sup>	0.242	1.6147	1.6529	3.2677	0.133

to 424 nm for pure PLA, due to increased density. Figure 7b highlights that tribological properties affected the PL behaviour, where samples at the lowest speed (0° orientation) demonstrated bright UV light irradiation (435 nm), suggesting enhanced mechanical performance of layered composites. The PL data support tribological and mechanical property observations, affirming that orientation during printing significantly influences printed sample performance.

The topological AFM images of PLA and PLA/CF are depicted in Figure 7c, showing no major differences in surface features between the two materials under various sliding speeds. However, Table 3 illustrates that surface roughness for both materials deteriorated as the sliding speed increased for the 0° printing orientation. For PLA (0°) samples, Sq data decreased by approximately 12% as the sliding speed increased from 0.8 to 1.2 m·s<sup>-1</sup>, likely due to heat generation that softened the PLA surface, as shown in Figure 4c. Table 3 also highlights that PLA/CF composites printed at 90° had lower Sq and Sa values compared to those printed at 0°, indicating that there is more fibre breakage during sliding at 0° samples, which hardening and enhanced interbonding, resulting in a rougher surface than at 90°. Interestingly, PLA demonstrated a rougher surface structure than PLA/CF, contradicting typical expectations, as fibre addition often leads to a rougher composite surface due to fibre breakage at the printing layup edges. However, this study successfully fabricated in-house filament with excellent surface roughness characteristics, achieving a 58% improvement for the 0° orientation. This

improvement was attributed to controlling the fibre alignment during filament fabrication, which enabled better bonding within printed layups and allowed the polymer matrix to coat the fibres effectively during extruding. Consequently, the filament was smoothly printed into samples with minimum surface roughness values between 0.049 and 0.0957  $\mu$ m, which were lower than those of PLA/CF at 90°. The higher surface roughness at 90° was due to the perpendicular fibre orientation relative to the applied load, which increased breakage and roughness.

# 3.4 Mechanical performance of printed samples at 0° orientation

Earlier results demonstrate that 0° printing orientation significantly enhances the tribological performance in printed samples. Therefore, a detailed analysis was conducted to evaluate the mechanical performance of the sample, as presented in Figures 8 and 9, by using PA as a reference sample. It was observed that the samples in the flexural test experienced a drastic reduction in performance at elevated temperatures (>30°C), as shown in Figure 8a. This reduction was attributed to the softening of the polymer matrix at higher temperatures, leading to a nearly complete (~100%) loss of mechanical strength. Additionally, Figure 8b illustrates that at 30°C, PLA in-house samples ruptured primarily due to fibre buckling, while at 55°C and 80°C, the samples elongated more before

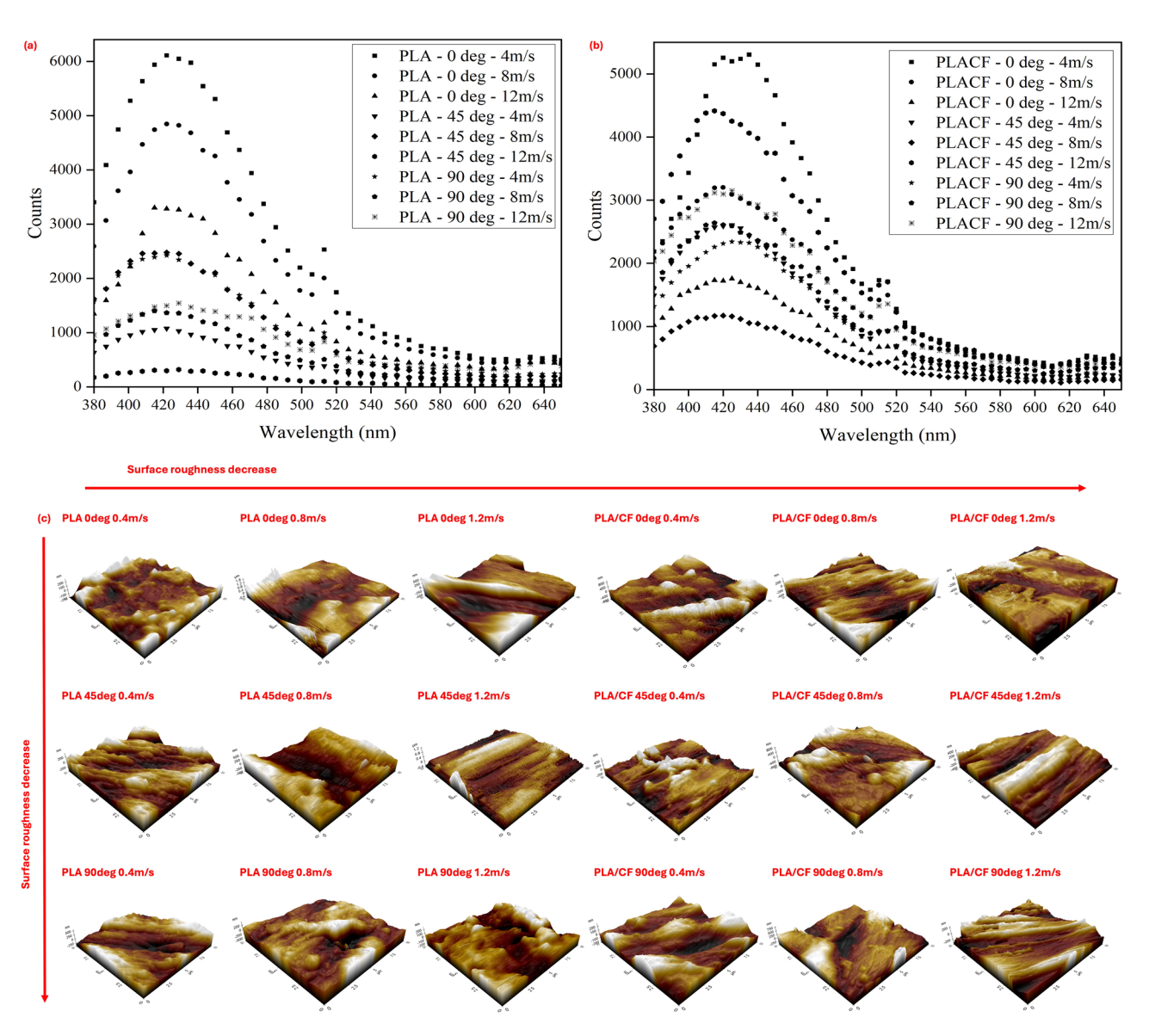


**Figure 7:** Emission spectra of filament prepared at 0°, 45°, and 90° for (a) PLA and (b) PLA/CF under different sliding speeds of 0.4, 0.8, and 1.2 m·s<sup>-1</sup>; 3D topographical AFM image of (c) PLA and PLA/CF at various sliding speeds and printing orientations.

Table 4: Printed filament density at different layer heights

Samples	Layer height (mm)	Density (g·cm <sup>−3</sup> )
PLA	0.1	1.172 ± 0.010
	0.2	1.155 ± 0.008
	0.3	1.142 ± 0.007
	0.1	1.342 ± 0.008
PLA/CF	0.2	1.325 ± 0.011
	0.3	1.292 ± 0.009

failure, highlighting the effect of temperature on deformation behaviour. Despite this limitation at higher temperatures, the flexural strength in Figure 8a indicated an improvement of up to 34% when comparing in-house fabricated PLA to conventional PLA. The in-house filament fabrication and printed sample process involves a controlled extrusion speed of 3.6 rpm and distinct temperature profiles of 170°C, 190°C, 180°C, and 110°C across four heating zones, ensuring precise fibre alignment and improved interfacial bonding. This led to a ~138% enhancement in flexural modulus based on Figures 8a-1 compared to conventional PLA. Additionally, the mechanical performance of the samples could not be accurately assessed at temperatures exceeding 40°C due to challenges in maintaining their structural integrity during testing. Consequently, the data were primarily obtained at room temperature, as testing beyond 40°C was constrained by these limitations. The performance decreased with

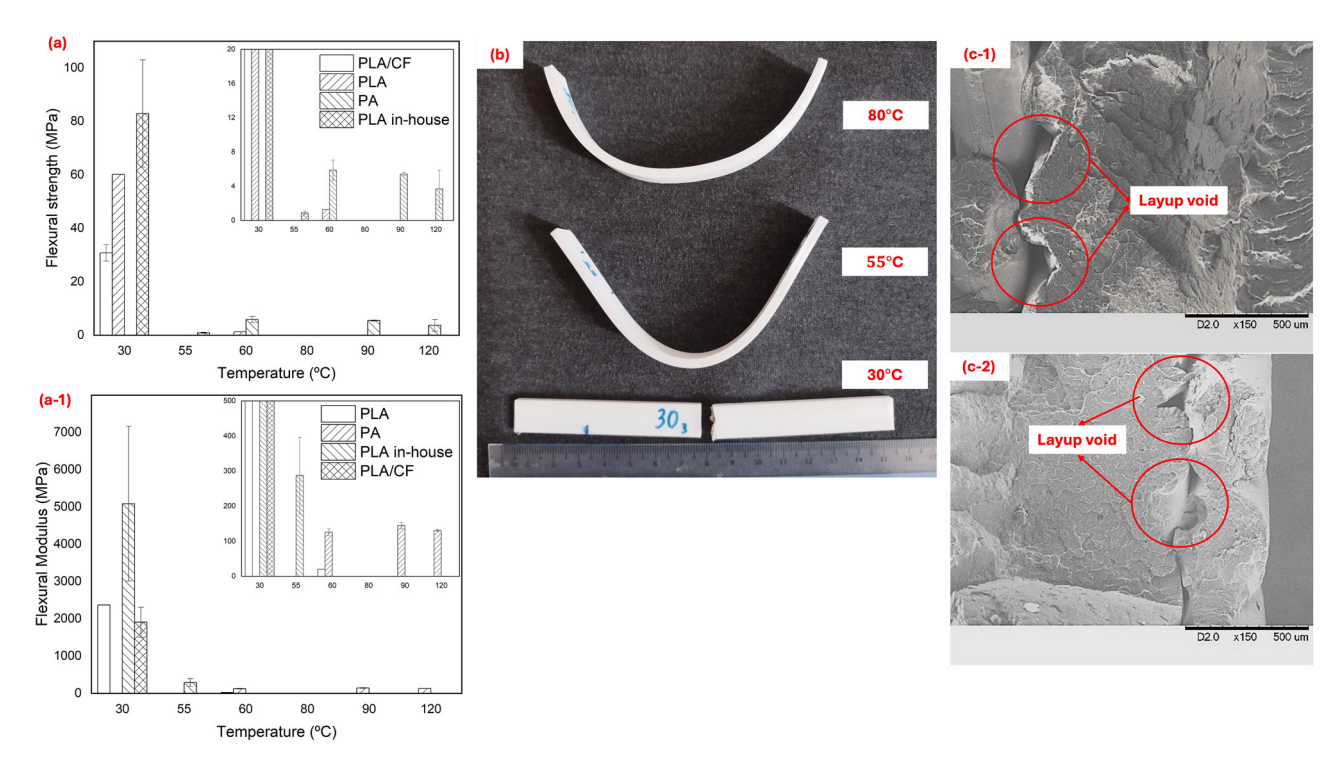
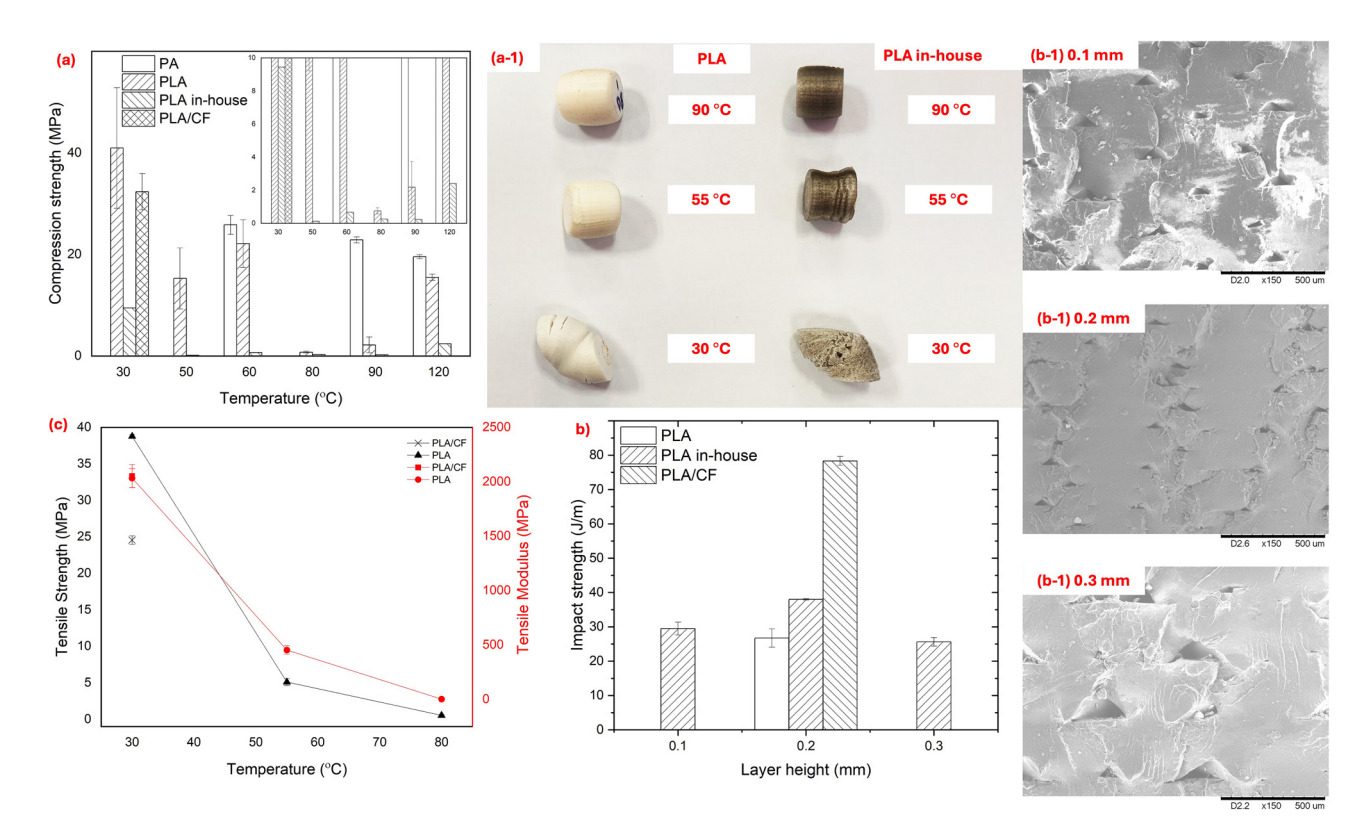


Figure 8: Flexural test of PA (reference samples), PLA, PLA in-house and PLA/CF in terms of (a) flexural strength and (a-1) flexural modulus, (b) deformation of PLA in-house samples at different temperatures; micrograph images of (c-1) PLA and (c-2) PLA in-house.



**Figure 9:** (a) Compressive test of PA, PLA, PLA in-house, and PLA/CF as well as their (a-1) observation using optical microscope images at various temperatures (30°C, 55°C, and 90°C), (b) impact test results of PLA, PLA in-house and PLA/CF at different layer heights during printing, (b-1) micrograph images of PLA in-house at various layer heights, and (c) tensile strength results of PLA in-house and PLA/CF composites.

increasing temperature due to polymer softening, which induced slipping during the testing process (32). In addition, the mechanical strength can be further enhanced through post-processing techniques, including heat treatment or drying (41).

Figure 8a and a-1 illustrate the comparative mechanical performance of PLA/CF composites, conventional PLA, and in-house PLA at various environmental temperature conditions. The in-house PLA showed a significant improvement of approximately 62% in flexural strength compared to PLA/CF composites, while conventional PLA achieved a 50% improvement. Similarly, the flexural modulus demonstrated an improvement of 22% for conventional PLA and an impressive ~177% for in-house PLA compared to PLA/CF composites, as shown in Figures 8a-1. These results highlight the superior bonding between the dispersion materials achieved in the in-house fabrication process. It has been established that the addition of fillers, such as short glass fibres, does not directly enhance the mechanical strength of composites (42). Conversely, excess fibre content, as noted in PLA/CF composites, resulted in decreased interlaminar bonding, thereby reducing composite strength (43). Figure 8c emphasizes the microstructural differences between PLA and in-house PLA. Figure 8c-1 and c-2 shows reduced void formation in in-house PLA, which indicates better layup during printing. In contrast, conventional PLA exhibited noticeable voids and inconsistencies in the layup sequence, which can weaken the material under applied loads. Furthermore, the interface between printed layers critically influences the macroscopic response of composites under load. The controlled printing orientation of inhouse PLA effectively enhanced anisotropy and strengthened interlayer interfaces, contributing to the observed improvement in mechanical performance (44).

The compression test results are presented in Figure 9a and a-1, highlighting contrasting outcomes compared to flexural strength. At 30°C, a 75% difference in compressive strength is evident between PLA (9 MPa) and in-house PLA (40 MPa), attributed to the inability of conventional PLA to withstand axial loads, resulting in buckling. This weakness arises from printed layers experiencing delamination under compression, a phenomenon more pronounced compared to bending in the flexural test, which resulted in lower compressive strength. The delamination and void formation under compression between PLA and PLA inhouse, shown in Figure 9a-1, become more prominent at 30°C due to crack propagation and filament breakage, which further reduces compression strength. As the temperature increases to 90°C, delamination decreases marginally, resulting in minimal differences in compressive strength, as recorded in Figure 9a. At elevated

temperatures (55°C and 90°C), both samples exhibit similar trends because they experienced delamination, with filament breakage and slip contributing to compressive strength reduction.

Therefore, the tensile strength performance of the samples was analysed, as shown in Figure 9c. The PLA in-house samples exhibited better tensile strength compared to PLA/CF composites. This difference is attributed to the influence of CF reinforcement, which introduces an aspect ratio filler that tends to cause fibre breakage during printing. This breakage is particularly prominent when fibres are printed on the sample surface, leading to weak interlayer bonding. Additionally, the presence of rough surfaces due to fibre alignment inconsistencies contributed to delamination and weakened the adhesion within the printed layers, which indicates the critical role of surface quality on mechanical performance (45). The samples were further examined for their impact strength under varying layer heights (0.1–0.3 mm), as depicted in Figure 9b. The results showed no significant difference in impact strength across different layer heights, with PLA in-house samples maintaining a consistent range of 30-40 MPa. However, micrograph images revealed distinct differences in layer morphology; only the 0.3 mm layer exhibited gaps between filaments, while the 0.1 and 0.2 mm layers were identical. The rapid cooling during printing allowed the layers to harden quickly, lowering the load applied at the top surface (46).

To enhance the mechanical and wear properties of 3Dprinted composites for specific applications, the selection of build orientation plays a crucial role. While the conventional approach emphasizes minimizing support structures during manufacturing, this study highlights that the choice of orientation should prioritize the desired material properties in specific loading directions. For example, a 0° orientation significantly enhances tensile and flexural strength due to the alignment of carbon fibres parallel to the loading direction, ensuring superior interfacial bonding. In contrast, a 45° orientation provides a balance between wear resistance and moderate mechanical performance, making it suitable for applications where multidirectional loading is expected. A 90° orientation, while exhibiting lower tensile properties due to weaker interlayer bonding, can be advantageous in scenarios where higher perpendicular wear resistance is required. These findings highlight the importance of tailoring build orientations based on application-specific requirements rather than manufacturability constraints alone. For instance, structural components subjected to uniaxial loads benefit from a 0° orientation, while functional parts requiring isotropic wear resistance may utilize 45° or 90° orientations.

# 3.5 Counterbalancing effects of different parameters

The interplay of temperature, build orientation, and CF composition was analysed to assess their influence on mechanical and wear properties. In terms of temperature, increased levels enhance interfacial bonding within the printed layers due to thermal softening, which facilitates better adhesion. However, beyond 55°C for PLA composites, the polymer matrix undergoes excessive softening. leading to reduced mechanical strength and wear resistance. Optimal results were observed at room temperature (~30°C), where mechanical integrity and wear resistance are maximized. Regarding the build orientation, samples printed at a 0° orientation exhibited superior mechanical strength and lower wear rates due to aligned CF reinforcement, which provides efficient load transfer and minimizes fibre pull-out. Conversely, the 90° orientation showed increased wear and lower mechanical properties because the applied forces act perpendicular to fibre alignment, leading to weak interfacial bonding. While for CF composition, higher levels improve mechanical performance by reinforcing the polymer matrix. However, excessive CF loading (above 9 wt%) disrupts network structures and increases material brittleness, adversely affecting wear resistance. The 9 wt% CF composition demonstrated optimal performance, balancing enhanced mechanical properties with manageable wear resistance. Through the comparative analysis, a unified parameter set was evaluated for its capability to achieve desirable performance across all properties. By using a room temperature of 30°C, a 0° build orientation, and 9 wt% CF composition, it ensures high tensile and flexural strength, optimal wear resistance, and a balance of tribological performance. Samples printed with these parameters demonstrated consistent behaviour, as evidenced by superior results in tensile strength (~75% improvement) and reduced wear rates compared to other configurations.

#### 4 Conclusion

In-house filaments tailored to control mechanical performance were fabricated by altering the fibre orientation within the filament through parameter control. By precisely managing filament parameters, including extrusion temperature (< $T_g$ ) and a drying duration of 5 h, the fibres were effectively oriented in specific directions within the filament. This internal alignment enhanced adhesion bonding between printed layers, as confirmed by micrograph imaging

without the fibres protruding on the filament surface. Furthermore, the controlled fibre alignment enabled seamless printing in dedicated printing orientations. Among these, the 0° printing orientation demonstrated excellent mechanical properties and tribological performance. This was attributed to the interlayer fibre breaking during printing, which hardened and improved the interfacial bonding. Key findings include

- i. In-house fabricated PLA filament demonstrated the presence of layup gaps within the printed layers, which were attributed to poor adhesion and interfacial bonding. In contrast, the in-house fabricated PLA/CF filament successfully aligned fibres in the 0° direction, enabling the filament to be printed at a dedicated printing orientation.
- ii. Rheological analysis indicated that the optimum fibre composition is 9 wt% of CF, which provided excellent dispersion and flowability, ensuring better interfacial bonding. Therefore, this composition was tested for tribological and mechanical performance. The increased in sliding speed led to material heating and subsequent softening, resulting in a higher coefficient of friction.
- iii. Mechanical testing demonstrated significant improvements for in-house PLA in flexural strength (~62% increment) and compression strength (~75% improvement) compared to conventional PLA and PLA/CF. The minimized layup gaps and voids in in-house filaments were key contributors to these enhancements. Additionally, impact strength performance ranged between 30 and 40 MPa at a layer height of 0.2 mm. Increased layer height to 0.3 mm resulted in poor adhesion due to rapid cooling of the subsequent layers, forming a large triangular shape.
- iv. This procedure can be extended to evaluate other filament types, such as PETG or ABS, to enhance wear and mechanical performance. Future research should focus on comparing the mechanical and tribological properties of various materials under different fibre orientations and conditions to further advance the application of 4D printing in engineering and manufacturing contexts.

The filament-making process contributes to the smooth structure of printed samples. Therefore, it is important to note that the samples must be dried for a minimum of 5 h before being extruded into filament and then dried again before the printing process. Due to these limitations, maintaining the performance of printed samples under optimal conditions is challenging, as the filament becomes fragile upon moisture absorption.

**Acknowledgments:** The authors acknowledge Fundamental Research Grant Scheme (FRGS), grant number FRGS/1/2024/TK10/UKM/02/3, funded by the Ministry of Higher Education (MOHE), Malaysia, and part of this research is supported by the Faculty of Engineering and Build Environment & Centre for Research and Instrumentation Management (CRIM), Universiti Kebangsaan Malaysia, grant number Dana Pecutan Penerbitan FKAB. The authors would also like to thank Final Year Project's students Sashwin Raj and Iswaran for their contribution to the experimental validation.

Funding information: The authors acknowledge the Fundamental Research Grant Scheme (FRGS), grant number FRGS/1/2024/TK10/UKM/02/3, funded by the Ministry of Higher Education (MOHE), Malaysia, and part of this research is supported by the Faculty of Engineering and Build Environment & Centre for Research and Instrumentation Management (CRIM), Universiti Kebangsaan Malaysia, grant number Dana Pecutan Penerbitan FKAB. The authors would also like to thank Final Year Project's students Sashwin Rai and Iswaran for their contribution to the experimental validation.

Author contributions: Writing – original draft: Nabilah Afiqah Mohd Radzuan. Writing – review & editing: Nabilah Afigah Mohd Radzuan & Izzat Mat Samudin. Methodology: Nabilah Afiqah Mohd Radzuan, Sashwin Raj & Iswaran. Supervision: Mohammad Reza Vaziri Sereshk, Quanjin Ma, Abu Bakar Sulong, Farhana Mohd Foudzi, Nishata Royan Rajendran Royan.

**Conflict of interest:** Authors state no conflict of interest.

**Data availability statement:** The datasets generated and/or analysed during the current study are available from the corresponding author on reasonable request.

#### References

- Allum J, Moetazedian A, Gleadall A, Silberschmidt VV. Interlayer bonding has bulk-material strength in extrusion additive manufacturing: New understanding of anisotropy. Addit Manuf. 2020;34(June):101297. doi: 10.1016/j.addma.2020.101297.
- Allum J, Moetazedian A, Gleadall A, Mitchell N, Marinopoulos T, McAdam I, et al. Extra-wide deposition in extrusion additive manufacturing: A new convention for improved interlayer mechanical performance. Addit Manuf. 2023;61:103334. doi: 10.1016/j.addma.2022.103334.
- McLouth TD, Severino JV, Adams PM, Patel DN, Zaldivar RJ. The impact of print orientation and raster pattern on fracture

- toughness in additively manufactured ABS. Addit Manuf. 2017;18:103-9. doi: 10.1016/j.addma.2017.09.003.
- Grejtak T, Jia X, Cunniffe AR, Shi Y, Babuska TF, Pack RC, et al. (4) Whisker orientation controls wear of 3D-printed epoxy nanocomposites. Addit Manuf. 2020;36:101515. doi: 10.1016/j. addma.2020.101515.
- Man Z, Wang H, He Q, Kim DE, Chang L. Friction and wear behaviour of additively manufactured continuous carbon fibre reinforced PA6 composites. Compos Part B: Eng. 2021;226:109332. doi: 10.1016/j.compositesb.2021.109332.
- Ji R, Zhao Q, Zhao L, Liu Y, Jin H, Wang L, et al. Study on high wear (6) resistance surface texture of electrical discharge machining based on a new water-in-oil working fluid. Tribol Int. 2023;180:108218. doi: 10.1016/i.triboint.2023.108218.
- Sun J, Wang L, Li J, Li F, Fang Y. An on-line imaging sensor based on magnetic deposition and flowing dispersion for wear debris feature monitoring. Mech Syst Signal Process. 2024;212:111321. doi: 10.1016/j.ymssp.2024.111321.
- Jia Z, Wang Q, Liu J. An investigation of printing parameters of independent extrusion type 3D print continuous carbon fiberreinforced PLA. Appl Sci. 2023;13(7):4222. doi: 10.3390/ app13074222.
- Zhang K, Zhang H, Wu J, Chen J, Yang D. Improved fibre placement (9) in filament-based 3D printing of continuous carbon fibre reinforced thermoplastic composites. Compos Part A: Appl Sci Manuf. 2023;168:107454. doi: 10.1016/j.compositesa.2023.107454.
- Nigam A, Tai BL. Surface characterization of three-dimensional printed fiber-reinforced polymer following an in-process mechanical-chemical finishing method. J Manuf Sci Eng. 2023;145(8):1-10. doi: 10.1115/1.4062146.
- Balamurugan K, Venkata Pavan M, Ahamad Ali SK, Kalusuraman G. Compression and flexural study on PLA-Cu composite filament using FDM. Materials Today: Proceedings. Elsevier Ltd; 2021. p. 1687-91. doi: 10.1016/j.matpr.2020.11.858.
- (12) Zolfaghari A, Purrouhani MR, Zolfagharian A. A response surface methodology study on 4D printing for layered PLA/TPU structures. Prog Addit Manuf. 2025;10:159-70. doi: 10.1007/s40964-024-00611-2.
- Rahmatabadi D, Soltanmohammadi K, Aberoumand M, Soleyman E. Ghasemi I. Baniassadi M. et al. 4D printing of porous PLA-TPU structures: effect of applied deformation, loading mode and infill pattern on the shape memory performance. Phys Scr. 2024;99(2):1-12. doi: 10.1088/1402-4896/ad1957.
- Lee WH, Alshebly YS, Ali MSM, Nafea M. Pattern-driven 4D printed PLA actuators. 8th IEEE International Conference on Smart Instrumentation, Measurement and Applications, ICSIMA. Institute of Electrical and Electronics Engineers Inc.; 2022. p. 116-21. doi: 10. 1109/ICSIMA55652.2022.9928870.
- Cicala G, Giordano D, Tosto C, Filippone G, Recca A, Blanco I. Polylactide (PLA) filaments a biobased solution for additive manufacturing: Correlating rheology and thermomechanical properties with printing quality. Materials. 2018;11(7):1-13. doi: 10.3390/ma11071191.
- Kingman J, Dymond MK. Fused filament fabrication and water contact angle anisotropy: The effect of layer height and raster width on the wettability of 3D printed polylactic acid parts. Chem Data Collect. 2022;40:100884. doi: 10.1016/j.cdc.2022.100884.
- Saleh M, Anwar S, Al-Ahmari AM, AlFaify AY. Prediction of mechanical properties for carbon fiber/PLA composite lattice structures using mathematical and ANFIS models. Polymers. 2023;15(7):1-27. doi: 10.3390/polym15071720.

- (18) He L, Chen B, Liu Q, Chen H, Li H, Chow WT, et al. A quasiexponential distribution of interfacial voids and its effect on the interlayer strength of 3D printed concrete. Addit Manuf. 2024;89:104296. doi: 10.1016/j.addma.2024.104296.
- (19) Xue R, Yuan P, Zhao B, Jing F, Kou X, Yue W, et al. DLP printing of BT/HA nanocomposite ceramic scaffolds using low refractive index BT crystals. J Materiomics. 2024;10(5):1036–48. doi: 10.1016/j.jmat. 2023.11.004.
- (20) Kiendl J, Gao C. Controlling toughness and strength of FDM 3D-printed PLA components through the raster layup. Compos Part B: Eng. 2020;180:107562. doi: 10.1016/j.compositesb.2019.107562.
- (21) Jayanth N, Jaswanthraj K, Sandeep S, Mallaya NH, Siddharth SR. Effect of heat treatment on mechanical properties of 3D printed PLA. J Mech Behav Biomed Mater. 2021;123. doi: 10.1016/j.jmbbm.2021.104764.
- (22) Hadi A, Kadauw A, Zeidler H. The effect of printing temperature and moisture on tensile properties of 3D printed glass fiber reinforced nylon 6. Materials Today: Proceedings. Elsevier Ltd; 2023. p. 48–55. doi: 10.1016/j.matpr.2023.04.641.
- (23) Guessasma S, Belhabib S, Nouri H. Effect of printing temperature on microstructure, thermal behavior and tensile properties of 3D printed nylon using fused deposition modeling. J Appl Polym Sci. 2021;138(14):1–15. doi: 10.1002/app.50162.
- (24) Akman R, Ramaraju H, Moore S, Verga A, Hollister SJ. Manufacture dependent differential biodegradation of 3D printed shape memory polymers. Virtual Phys Prototyp. 2024;19(1):1–14. doi: 10. 1080/17452759.2024.2371504.
- (25) Bokharaie BU, Aghababaei R, Dias MA, Budzik MK. Failure of 3D-printed composite continuous carbon fibre hexagonal frames. Compos Part B: Eng. 2024;275:111307. doi: 10.1016/j.compositesb. 2024.111307.
- (26) Mohd Radzuan NA, Khalid NN, Foudzi FM, Rajendran Royan NR, Sulong AB. Mechanical analysis of 3D printed polyamide composites under different filler loadings. Polymers. 2023;15(8):1846. doi: 10.3390/polym15081846.
- (27) Radzuan NAM, Foudzi FM, Sulong AB, Al-Furjan MSH, Royan NRR. Quick insight into the dynamic dimensions of 4D printing in polymeric composite mechanics. Rev Adv Mater Sci. 2024;63(1):1–12. doi: 10.1515/rams-2024-0011.
- (28) Khalid NN, Mohd Radzuan NA, Sulong AB, Mohd Foudzi F, Hui D. Adhesion behaviour of 3D printed polyamide–carbon fibre composite filament. Rev Adv Mater Sci. 2022;61(1):838–48. doi: 10.1515/ rams-2022-0281.
- (29) Zhiani Hervan S, Altınkaynak A, Parlar Z. Hardness, friction and wear characteristics of 3D-printed PLA polymer. Proc Inst Mech Eng, J: J Eng Tribol. 2021;235(8):1590–8. doi: 10.1177/ 1350650120966407.
- (30) Karunanithi C, Natarajan S. Surface characteristics of 3D printed PEEK polymer using atomic force microscopy. J Mech Behav Biomed Mater. 2024;149:106237. doi: 10.1016/j.jmbbm.2023.106237.
- (31) Das A, Gilmer EL, Biria S, Bortner MJ. Importance of polymer rheology on material extrusion additive manufacturing: correlating process physics to print properties. ACS Appl Polym Mater. 2021;3:1218–49. doi: 10.1021/acsapm.0c01228.
- (32) Mohd Radzuan NA, Khalid NN, Foudzi FM, Rajendran Royan NR, Sulong AB. Mechanical analysis of 3D printed polyamide composites under different filler loadings. Polymers. 2023;15(8):1846. doi: 10.3390/polym15081846.

- (33) Wozniak M, Rylski A, Lason-Rydel M, Orczykowska M, Obraniak A, Siczek K. Some rheological properties of plastic greases by Carreau-Yasuda model. Tribol Int. 2023;183:108372. doi: 10.1016/j. triboint.2023.108372.
- (34) Li B, Chen G, Zhang H, Sheng C. Development of non-isothermal TGA-DSC for kinetics analysis of low temperature coal oxidation prior to ignition. Fuel. 2014;118:385–91. doi: 10.1016/j.fuel.2013.11.011.
- (35) Zakaria MY, Sulong AB, Sahari J, Suherman H. Effect of the addition of milled carbon fiber as a secondary filler on the electrical conductivity of graphite/epoxy composites for electrical conductive material. Compos Part B: Eng. 2015;83:75–80. doi: 10.1016/j. compositesb.2015.08.034.
- (36) Dickson AN, Dowling DP. Enhancing the bearing strength of woven carbon fibre thermoplastic composites through additive manufacturing. Compos Struct. 2019;212:381–8. doi: 10.1016/j. compstruct.2019.01.050.
- (37) Hou Z, He J, Tian X, Zhu W, Wang C, Liu P, et al. Performance and failure modes of continuous fibre-reinforced energy absorption tubes by cylindrical layered 3D printing. Virtual Phys Prototyping. 2024;19(1):1–19. doi: 10.1080/17452759.2024.2367122.
- (38) Hanon MM, Zsidai L. Comprehending the role of process parameters and filament color on the structure and tribological performance of 3D printed PLA. J Mater Res Technol. 2021;15:647–60. doi: 10.1016/j.jmrt.2021.08.061.
- (39) Kothavade PA, Yadav P, Nidhankar AD, Torris A, Pol H, Kafi A, et al. Luminescent 3D printed poly(lactic acid) nanocomposites with enhanced mechanical properties. Polym Eng Sci. 2023;63(7):2059–72. doi: 10.1002/pen.26345.
- (40) Wan M, Jiang X, Nie J, Cao Q, Zheng W, Dong X, et al. Phosphor powders-incorporated polylactic acid polymeric composite used as 3D printing filaments with green luminescence properties. J Appl Polym Sci. 2020;137(18):48644. doi: 10.1002/app.48644.
- (41) Pazhamannil RV, Govindan P, Edacherian A, Hadidi HM. Impact of process parameters and heat treatment on fused filament fabricated PLA and PLA-CF. Int J Interact Des Manuf. 2024;18(4):2199–213. doi: 10.1007/s12008-022-01082-x.
- (42) Mohankumar HR, Benal MGM, Pradeepkumar GS, Tambrallimath V, Ramaiah K, Khan TMY, et al. Effect of short glass fiber addition on flexural and impact behavior of 3D printed polymer composites. ACS Omega. 2023;8(10):9212–20. doi: 10.1021/acsomega.2c07227.
- (43) Xin Z, Ma Y, Chen Y, Wang B, Xiao H, Duan Y. Fusion-bonding performance of short and continuous carbon fiber synergistic reinforced composites using fused filament fabrication. Compos Part B: Eng. 2023;248:110370. doi: 10.1016/j.compositesb.2022. 110370.
- (44) Zorzetto L, Andena L, Briatico-Vangosa F, De Noni L, Thomassin JM, Jérôme C, et al. Properties and role of interfaces in multimaterial 3D printed composites. Sci Rep. 2020;10(1):1–17. doi: 10.1038/ s41598-020-79230-0.
- (45) Radzuan NAM, Sulong AB, Verma A, Muhamad N. Layup sequence and interfacial bonding of additively manufactured polymeric composite: A brief review. Nanotechnol Rev. 2021;10(1):1853–72. doi: 10.1515/ntrev-2021-0116.
- (46) Faes M, Ferraris E, Moens D. Influence of inter-layer cooling time on the quasi-static properties of ABS components produced via fused deposition modelling. Procedia CIRP. 2016;42(Isem Xviii):748–53. doi: 10.1016/j.procir.2016.02.313.